http://dx.doi.org/10.5516/NET.02.2014.011

# PUMP DESIGN AND COMPUTATIONAL FLUID DYNAMIC ANALYSIS FOR HIGH TEMPERATURE SULFURIC ACID TRANSFER SYSTEM

JUNG-SIK CHOI[1], YOUNG-JOON SHIN[2], KI-YOUNG LEE[2], YONG-SUP YUN[3], and JAE-HYUK CHOI[3*]
[1]Graduate school of Korea Maritime and Ocean University,
727 Taejong-ro, Yeongdo-Gu, Busan, Korea.
[2]Korea Atomic Energy Research Institute,
Daedeok-Daero 989-111, Yuseong-Gu, Daejeon, Korea.
[3]Division of Marine Engineering System Korea Maritime and Ocean University,
727 Taejong-ro, Yeongdo-Gu, Busan, Korea.
[*]Corresponding author. E-mail : choi_jh@kmou.ac.kr

*Received January 24, 2014*
*Accepted for Publication April 24, 2014*

In this study, we proposed a newly designed sulfuric acid transfer system for the sulfur-iodine (SI) thermochemical cycle. The proposed sulfuric acid transfer system was evaluated using a computational fluid dynamics (CFD) analysis for investigating thermodynamic/hydrodynamic characteristics and material properties. This analysis was conducted to obtain reliable continuous operation parameters; in particular, a thermal analysis was performed on the bellows box and bellows at amplitudes and various frequencies (0.1, 0.5, and 1.0 Hz). However, the high temperatures and strongly corrosive operating conditions of the current sulfuric acid system present challenges with respect to the structural materials of the transfer system. To resolve this issue, we designed a novel transfer system using polytetrafluoroethylene (PTFE, Teflon®) as a bellows material for the transfer of sulfuric acid. We also carried out a CFD analysis of the design. The CFD results indicated that the maximum applicable temperature of PTFE is about 533 K (260 °C), even though its melting point is around 600 K. This result implies that the PTFE is a potential material for the sulfuric acid transfer system. The CFD simulations also confirmed that the sulfuric acid transfer system was designed properly for this particular investigation.

KEYWORDS : High Temperature Sulfuric Acid Transfer System, Sulfur-Iodine (SI) Cycle, Sulfuric Acid Decomposition, Hydrogen Production, Computational Fluid Dynamics (CFD)

## 1. INTRODUCTION

Among various hydrogen production technologies, steam reforming technology is responsible for producing ~90 % of the hydrogen used in recent years [1]. This method is the most common process for producing commercial bulk hydrogen at high temperatures (700-1100 °C) under various conditions. However, the steam reforming technology utilizes fossil fuels and therefore does not prevent carbon dioxide from being released into the atmosphere. Among various hydrogen production technologies that do not utilize fossil fuels, nuclear hydrogen is the most likely candidate for commercialization.

There are currently over 400 nuclear hydrogen production cycles proposed. Nuclear hydrogen production cycles, and the sulfur-iodine (SI) thermochemical cycle have attracted much attention recently because its theoretical heat transfer efficiency for hydrogen is above 50 % [2]. The Japan Atomic Energy Research Institute (JAERI) has been involved in the study of the SI thermochemical hydrogen production cycle [3-5], which was originally proposed by General Atomics [6].

The SI thermochemical cycle consists of three chemical reactions that result in dissociation of water into hydrogen and oxygen;

(a) Bunsen reaction :
$$I_2 + SO_2 + 2H_2O \rightarrow 2HI + H_2SO_4 \quad (T \sim 120\ ^\circ C)$$
(b) Sulfuric acid decomposition :
$$H_2SO_4 \rightarrow SO_2 + H_2O + 1/2O_2 \quad (T > 800\ ^\circ C)$$
(c) Hydriodic acid decomposition :
$$2HI \rightarrow I_2 + H_2 \quad (T > 350\ ^\circ C)$$

Net $H_2O \rightarrow H_2 + 1/2O_2$

As shown above, the chemical reaction can be represented as the Bunsen reaction (a), the sulfuric acid decomposition reaction (b), and the hydriodic acid decomposition reaction (c).

Extensive experimental and theoretical research has been carried out worldwide over the last decade to investigate the potential of these hydrogen production processes [7-9]. However, much of the research has focused on the development of supplementations to address specific problems associated with this process [10-17]. For the

sulfuric acid concentration/decomposition reaction, challenges involving material corrosion in the presence of a high temperature energy source emerged and investigations on catalyst activity and stability were subsequently carried out [10-14]. Onuki *et al*. [14] determined that material resistance was crucial for the development of the hydriodic acid concentration/decomposition reaction. The sulfuric acid decomposition reaction takes place at high temperatures and is catalyzed by an expensive metal catalyst. This reaction requires the highest temperature during the thermochemical hydrogen production process and therefore dictates the temperature requirement of the primary energy source [15]. To improve these problems, Giaconia *et al.* [16] investigated the bunsen reaction and evaluated the effects of various operation parameters on the product phase behavior. Goldstein *et al*. [17] identified an upper limit and estimated the ideal efficiency of the thermochemical SI process when used in conjunction with a high temperature reactor.

A device that can be used to transfer sulfuric acid at high temperatures during the SI process is shown in Fig. 1. The pump used to carry sulfuric acid during the SI process is a very important piece of equipment. According to the SI process flow sheet [18], to transfer sulfuric acid to a vaporizer of a sulfuric acid decomposer at a gauge pressure of 0.1 atm, the sulfuric acid should be cooled to 177 °C or instead of the vaporizer of a multistage distillation column. Some of the disadvantages associated with the sulfuric acid transfer system include the risk of handling and the reduced efficiency which is caused by the transfer, re-heating, and pressurization of the sulfuric acid. The thermal stability of the materials used in the sulfuric acid decomposition reaction is also an important consideration because the hot sulfuric acid produces harsh chemical environments during the reaction.

Generally, a ceramic piston pump is used to transfer sulfuric acid. The ceramic is used as a piston material and its fluid limitation temperature is less than 115 °C [19]. Therefore, it is necessary to improve the inner material used for transferring hot sulfuric acid within the pump. However, research regarding the use of proper materials in this pump for transferring sulfuric acid has been very limited thus far.

In this study, we proposed a novel sulfuric acid transfer system for the SI thermochemical cycle. Polytetrafluoroethylene (PTFE, Teflon®) [20] exhibits a coefficient of friction against polished steel in the range of 0.05 to 0.13, which is one of the lowest measured values for a solid. PTFE is a crystalline polymer, which is usable for a part working under a temperature lower than 533 K (260 °C), with a melting point of ~ 600 K (327 °C) [20]. This feature makes it suitable for applications that require reduced friction between two solid components, such as gears or moving parts. We proposed that PTFE could be used as the inner material of the sulfuric acid transfer system. The proposed sulfuric acid transfer system was evaluated using a computational fluid dynamics (CFD) analysis. To determine the thermodynamic/hydrodynamic characteristics and material properties [21], the CFD analysis was performed under similar conditions as those of actual driving processes by utilizing user-defined functions (UDFs) [22] with varying frequencies and amplitudes. In particular, by performing a thermal analysis on the bellows and bellows end-plate, the durability characteristics of the PTFE used on the moving parts during the continuous operation of the transfer system were evaluated.

## 2. MODELING AND CFD METHOD OF THE SULFURIC ACID TRANSER SYSTEM

### 2.1 Design Modeling

Fig. 1 (a) is shown as the concentration and decomposition steps of sulfuric acid in SI process [23]. In the dotted(·····) section, the process is illustrated to show that sulfuric acid is transferred from the multistage distillation column to a vaporizer using the sulfuric acid transportation system. The sulfuric acid transfer system previously suggested was presented in Fig. 1 (b). Due to the operation temperature limit of ceramic piston pumps, forced cooling was needed so the thermal efficiency was lowered in this system. In Fig. 1 (c), the process for sulfuric acid transportation was illustrated. The thermal efficiency is larger than in the previous system (Fig. 1 (b)) because the forced cooling was not required in our system.

Fig. 2 shows a schematic of our newly designed sulfuric acid transfer system and CFD analysis region. The pump parts and check valve in the sulfuric acid transfer system is presented in Fig. 2 (a), and the dimensions of the pump section and the calculated segments (bellows box, bellows, and bellows end-plate) of the system is shown in Fig. 2 (b). The pumping segment shown in Fig. 2 (a) consisted of a check valve (60), a bellows box (21, which is connected to the check valve), and a driving unit (23, which contracts /expands the bellows inside the bellows box). After a flow path with connecting the bellows box (21) and check valve (60) was established, the sulfuric acid solution from check valve introduced to bellows box (21) before being pumped to outside. The cooling water cooled the introducing inlet (42) of bellows (22) and discharging to outlet (44). For the expansion and contraction of the bellows (22), the piston (26) located in the actuator (23), moved the round trip in the cylinder (25) and provided the driving force. At this time, the reciprocating cycle of the piston was the frequency and the forward / backward amplitude of piston (26) was controlled by micrometer head (36).

When the bellows (22) was contracted by lowering the upper check ball, the check valve (60) closed the outlet flow, and the sulfuric acid was introduced to the bellows box (21) when the inlet flow path was opened with raising a lower check ball. When the bellows (22) was expanded, the flow path was opened by raising the

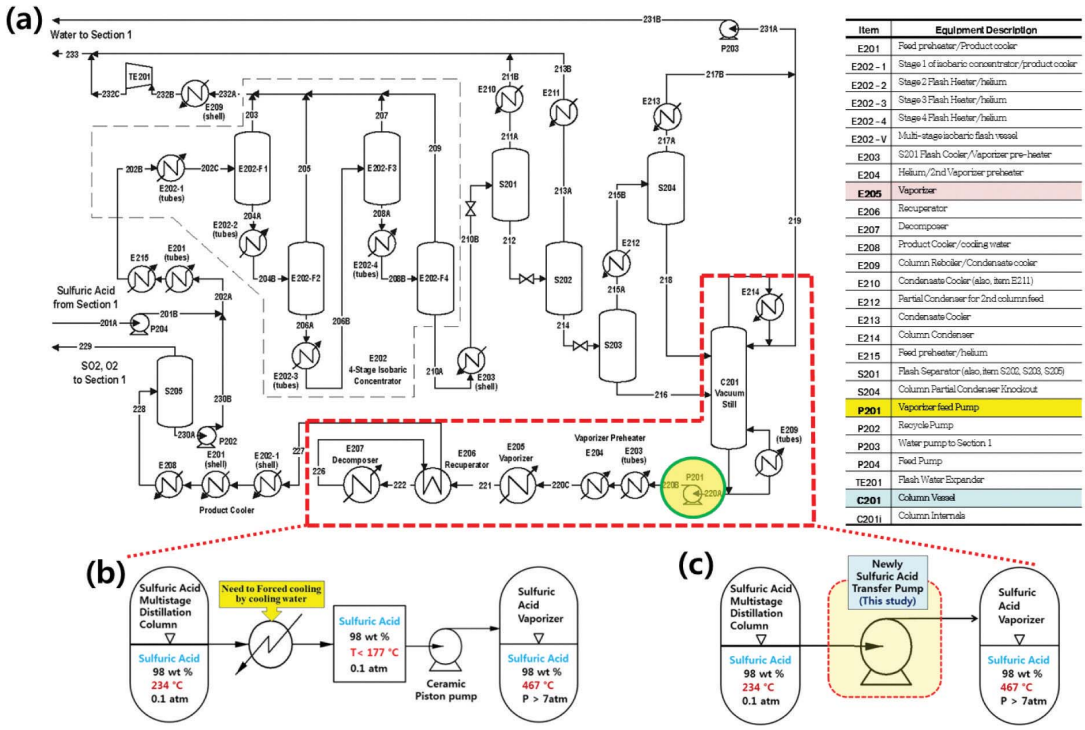


| Item | Equipment Description |
|---|---|
| E201 | Feed preheater/Product cooler |
| E202 - 1 | Stage 1 of isobaric concentrator/product cooler |
| E202 - 2 | Stage 2 Flash Heater/helium |
| E202 - 3 | Stage 3 Flash Heater/helium |
| E202 - 4 | Stage 4 Flash Heater/helium |
| E202 - V | Multi-stage isobaric flash vessel |
| E203 | S201 Flash Cooler/Vaporizer pre-heater |
| E204 | Helium/2nd Vaporizer preheater |
| **E205** | Vaporizer |
| E206 | Recuperator |
| E207 | Decomposer |
| E208 | Product Cooler/cooling water |
| E209 | Column Reboiler/Condensate cooler |
| E210 | Condensate Cooler (also, item E211) |
| E212 | Partial Condenser for 2nd column feed |
| E213 | Condensate Cooler |
| E214 | Column Condenser |
| E215 | Feed preheater/helium |
| S201 | Flash Separator (also, item S202, S203, S205) |
| S204 | Column Partial Condenser Knockout |
| **P201** | Vaporizer feed Pump |
| P202 | Recycle Pump |
| P203 | Water pump to Section 1 |
| P204 | Feed Pump |
| TE201 | Flash Water Expander |
| **C201** | Column Vessel |
| C201i | Column Internals |

Fig. 1. High Temperature Sulfuric Acid Transportation System in SI Cycle: (a) Process for Concentration and Decomposition of Sulfuric Acid, a Schematic Diagram for Sulfuric Acid Transportation Process using Ceramic Piston Pump (b), and Proposed in this Study (c).

check ball, and the sulfuric acid flowed out by closing inlet flow path. Therefore, when the bellows (22) was contracted, the sulfuric acid solution was transferred from the check valve (60) to bellows (22) in bellows box (21). When the bellows was expanded, the sulfuric acid was pumped from bellows box (21) to the check valve (60). By allowing water to flow inside the bellows, the bellows can be cooled and subsequently be able to maintain its temperature limit during continuous operation. Therefore, to satisfy this condition, PTFE was utilized as the material of the bellows because of its high acid resistance.

The CFD analysis was conducted to ascertain the reliability of continuous operation and the thermal analysis for the bellows box and the bellows as the sulfuric acid transfer rate changed. To simulate the proposed transfer system, we designed the calculated section for the CFD (numerical) analysis, as shown in Fig. 2 (b). The dimension of the bellows box was 600 mm (width) ×350 mm (height), while that of the bellows was 1 mm (thickness) ×247 mm (width) ×117 mm (height) with a span of 26 mm and a pitch (1/2) of 10 mm. The material was PTFE that was installed inside the bellows box under adiabatic conditions. The bellows end-plate was 3 mm thick ×117 mm long and composed of stainless steel (STS). The diameter of the entrance/exit ports for the cooling water was 10 mm and the diameter of the suction/discharging ports for sulfuric acid was 60 mm.

By reciprocating bellows, the flow rate of the pump for transferring 98 wt% sulfuric acid solution (density 1.8 g/cm) was determined by equation (1), but the flow rate of the sulfuric acid was changed according to frequency which was a single-variable in this study.

$$\mathbf{Q}\left(\frac{\mathbf{Nm^3}}{\boldsymbol{h}}\right) = \mathbf{A(m)} \times \frac{\mathbf{1}}{\mathbf{2}}\, \boldsymbol{Frequency(Hz)} \times \boldsymbol{\pi} \times \boldsymbol{d^2(m)} \qquad (1)$$

where, A is the amplitude of the bellows, the frequency (Hz) is 1/T (i.e.; T is the period of a cycle, sec), and d is the radius of the bellows.

## 2.2 CFD Analysis Methods and CFD Domain with Boundary Conditions

The FLUENT® code used the CFD analysis provided the UDFs, which is a useful method which can be used as users demand [22], so we applied the moving grid(dynamic mesh) using UDF to simulate the actual behavior of the pump for transferring sulfuric acid solution. The dynamic mesh model can be used to simulate fluid flows where the shape of the domain changes as a function of time due to the motion on the domain boundaries [24]. The dynamic mesh model can be applied to single or multiphase flows (and multi-species flows). Therefore, to describe the movement of the bellows more accurately, the dynamic mesh model in ANSYS FLUENT® Release 14.5 was applied to the simulation.

The CFD analysis was performed using the used-code of the finite volume method (FVM), which is the PISO pressure-velocity coupling scheme algorithm of ANSYS FLUENT® Release 14.5 to solve the governing equation. Additionally, the standard κ-ε model and the standard wall function were applied for turbulent flow analysis [24].

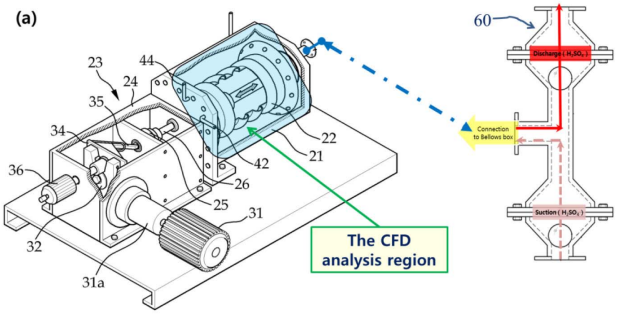


| No. | Description | No. | Description | No. | Description | No. | Description |
|---|---|---|---|---|---|---|---|
| 21 | Bellows Box | 25 | Cylinder | 32 | Worm | 36 | Micrometer Head |
| 22 | Bellows | 26 | Piston | 33 | Worm Wheel | 42 | Cooling Water Inlet |
| 23 | Actuator (Drive unit) | 31 | Motor | 34 | Plate Cam | 44 | Cooling Water Outlet |
| 24 | Gear Box | 31a | Motor Shaft | 35 | Cam Rotating Arm | 60 | Check Valve |

Fig. 2. A Schematic of Newly Designed Sulfuric Acid Transfer System: (a) Pump Section with Check valve, (b) A Dimension of the CFD Analysis Region.

**Table 1.** Physical Properties of the PTFE and STS

| | PTFE | STS |
|---|---|---|
| Material Type | Solid | Solid |
| Density (Kg/m$^3$) | 2.200x10$^3$ | 7.800x10$^3$ |
| Specific heat (J/Kg·K) | 1.500x10$^3$ | 5.000x10$^2$ |
| Thermal conductivity (W/m·K) | 2.500x10$^{-1}$ | 1.500x10$^1$ |

Fig. 3 shows the CFD domain with boundary conditions. The dynamic simulation was performed according to the different frequency (0.1 Hz, 0.5 Hz, and 1.0 Hz). The suction flow rates of sulfuric acid were changed with the different frequency. The values of sulfuric acid were 4.52 kg/s, 22.6 kg/s, and 45.2 kg/s for 0.1 Hz, 0.5 Hz, and 1.0 Hz, respectively. And, the flow rate of cooling water was fixed at 3.9 kg/s. The condition of bellows box was set at the value of the insulated wall, while the bellows and bellows end-plate were composed of PTFE and STS, respectively. In reality, all parts contacting the sulfuric acid need to be PTFE. Therefore, the bellows end-plate and the bellows box wall also need to be of PTFE or lined with PTFE.

Table 1 describes the physical properties of the PTFE and STS. The density of the PTFE was ~2.200 $\times 10^3$ (Kg/m$^3$) [25], the specific heat was 1.500 $\times 10^3$ (J/kg·K), and the thermal conductivity was 2.500 $\times 10^{-1}$ (W/m·K) [20]. The density of the STS was 7.800 $\times 10^3$ (Kg/m$^3$), the specific heat was 5.000 $\times 10^2$ (J/kg·K), and the thermal conductivity was 1.500 $\times 10^1$ (W/m·K) [26]. These characteristic values were applied equally for all frequencies.

In this investigation, various assumptions were considered to conduct the CFD analysis, such as:

1) The bellows box was completely insulated since the calculated domain could not exchange heat with the atmosphere,
2) The bellows box was completely filled with sulfuric acid (520.15 K), and
3) The bellows was completely filled with cooling water (298.15 K).

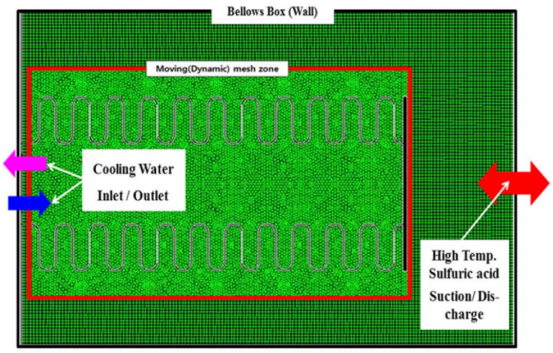


| Boundary | Characteristics |
|---|---|
| Sulfuric acid Suction | T = 520.15 K<br>Q = 4.52 kg/s (0.1 Hz)<br>Q = 22.6 kg/s (0.5 Hz)<br>Q = 45.2 kg/s (1.0 Hz) |
| Cooing Water Inlet | T = 298.15 K<br>Q = 3.9 kg/s |
| Frequency (Hz) | 0.1, 0.5, and 1.0 (3 cases) |
| Bellows Box | Adiabatic |
| Bellows with End-plate | Moving condition (refer to frequency) |

Fig. 3. The CFD Domain with Boundary Conditions.

## 3. RESULTS AND DISCUSSIONS

### 3.1 Simulation Results for the Inner PTFE Layer and Near the Bellows

Fig. 4 shows the temperature distribution of the inner bellows (PTFE) at various frequencies (0.1, 0.5, and 1.0 Hz). Data were recorded at 50, 100, 150, and 200 s for each frequency.

At 0.1 Hz (Fig. 4 (a)), the inside temperature distribution of the PTFE was in the range of 386-404 K at 50 s, 404-422 K at 100 s, and 409-420 K at 150 s and 200 s. Prior to 150 s, the maximum and minimum temperature was 422 K and 386 K, respectively. After 150 s, the maximum temperature was 420 K and the minimum temperature was 409 K. This temperature was then maintained without any significant change.

At 0.5 Hz (Fig. 4 (b)), the temperature distribution of PTFE was in the range of 386-404 K at 50 s, 404-422 K at 100 s, and 409-420 K at 150 s and 200 s. Prior to 150 s, the maximum and minimum temperature was 431 K and 398 K, respectively, and the maximum temperature difference for the inner PTFE was 33 K. After 150 s, the temperature difference between the maximum and minimum temperature was 11 K.

At 1.0 Hz (Fig. 4 (c)), the temperature distribution of the PTFE was 398-409 K at 50 s and 409-420 K at 100, 150, and 200 s. Prior to 100 s, the minimum temperature was 398 K and the maximum temperature was 420 K. After 100 s, temperature difference was 11 K with the maximum temperature of 420 K and the minimum temperature of 409 K.

Based on the calculated results in Fig. 4 (a) through Fig. 4 (c), it was confirmed that the temperature of the bellows (PTFE), which was measured periodically using reciprocating movements in the hot sulfuric acid (520.15 K, 98 wt%), did not significantly increase. This result may be explained by the fact that the water that was circulated within the bellows was able to properly absorb the heat transferred from the hot sulfuric acid facing the outer layer of the bellows. Based on the calculated results in Fig. 4, the time required to maintain a constant temperature within the inner bellows (PTFE) increased as the frequency decreased. However, after 150 s, a constant temperature distribution was exhibited at all frequencies.

Within the temperature range from 25 °C to 300 °C, the linear coefficient of expansion for PTFE was $2.2 \times 10^{-6}$ mm/mm °C [20]. Therefore, it was determined that no significant deformation occurred because of the contact with the hot sulfuric acid.

Fig. 5 shows the profiles of the temperature at the Neck and Pitch of the bellows at 200 s. The temperature was obtained by monitoring the area-weighted average of the total temperature every 1 s for each portion of the bellows. Fig. 5 (a) shows the temperature distribution of the Neck surface facing the sulfuric acid and Fig. 5 (b) shows the temperature distribution of the Neck surface facing the cooling water. Fig. 5 (c) shows the temperature distribution of the Pitch surface facing sulfuric acid and Fig. 5 (d) shows the temperature distribution of the Pitch surface facing the cooling water.

In Fig. 5 (a), the temperature of the contact surface of the Neck facing the sulfuric acid increased from 409 K to 467 K and was maintained at 467 ± 2 K under all simulated conditions (0.1, 0.5, and 1.0 Hz). The time required to reach 467 K was 119, 128, and 111 s at 0.1, 0.5, and 1.0 Hz, respectively.

In Fig. 5 (b), the temperature of the contact surface of the Neck facing the cooling water increased from 298 K to 349 K under every set of conditions, and the temperature was maintained at 349 ± 1 K. The time required to reach 349 K was 110, 116, and 107 s at 0.1, 0.5, and 1.0 Hz, respectively.

In Fig. 5 (c), the temperature of the contact surface of the Pitch facing the sulfuric acid increased from 409 K to 467 K and it was maintained at 467 ± 2 K. The time required to reach 467 K was 90, 89, and 91 s at 0.1, 0.5, and 1.0 Hz, respectively.

In Fig. 5 (d), the temperature of the contact surface of the Pitch facing the cooling water increased from 298

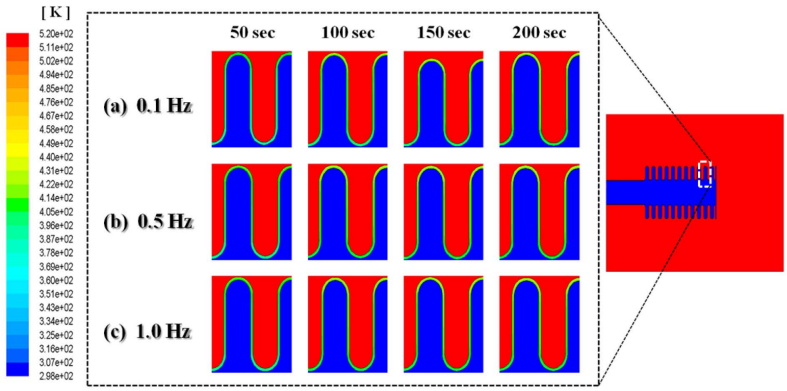


Fig. 4. Temperature Distribution of Inner Bellows (PTFE) for Frequency (0.1, 0.5, and 1.0 Hz).

K to 350 K and was maintained at 350 ± 1 K. The time required to reach 350 K was 106, 104, and 148 s at 0.1, 0.5, and 1.0 Hz, respectively.

As shown in Fig. 5 (a) and Fig. 5 (c), the time required for the temperature of the PTFE surface in contact with sulfuric acid to increase to 467 K and reach a constant was not affected by the frequency. However, the time required for the temperature to reach 467 K in Neck was 20-39 s faster than that in the Pitch. It was determined that the Pitch significantly contracted in the presence of sulfuric acid as evidenced by the reciprocation of the bellows.

In Fig. 5 (b) and Fig. 5 (d) at 0.1 Hz and 0.5 Hz, 110 s was required for the temperature of the PTFE surface in contact with the cooling water to increase to 350 K and reach a constant in both the Neck and the Pitch. However, at 1.0 Hz, 107 s and 148 s was required for the temperature to increase in the Neck and the Pitch, respectively. As the frequency increased, more reciprocating movements were generated. Consequently, the cooling water flowed in and out of the Pitch more easily as the frequency increased.

In this study, we incorporated PTFE into the bellows of an SI thermochemical cycle. PTFE is a crystalline polymer, which is usable for a part working under a temperature lower than 533 K (260 °C), with a melting points of ~ 600 K (327 °C) [20] and a density of ~2.200 $\times 10^{-3}$ Kg/m$^3$ [25]. The maximum temperature reached during the reaction was 467 K that is significantly lower than the melting point of PTFE. This result indicates that PTFE can be used as a structural material for the bellows within the sulfuric acid transfer pump for the SI process.

Fig. 6 shows the velocity vector inside the bellows box and the moving parts surrounding the bellows. Fig. 6 (a) shows the maximum expansion point and Fig. 6 (b) shows the maximum shrinkage point at each frequency (0.1, 0.5, and 1.0 Hz). At the maximum expansion point of the bellows (Fig. 6 (a)), the velocity inside the bellows box was in the range of 3.52 $\times 10^{-4}$ - 1.418 m/s and its distribution inside the bellows upon exposure to the cooling water was in the range of 3.52 $\times 10^{-4}$ - 3.78 m/s at 0.1 Hz. When the hot sulfuric acid was fully discharged,

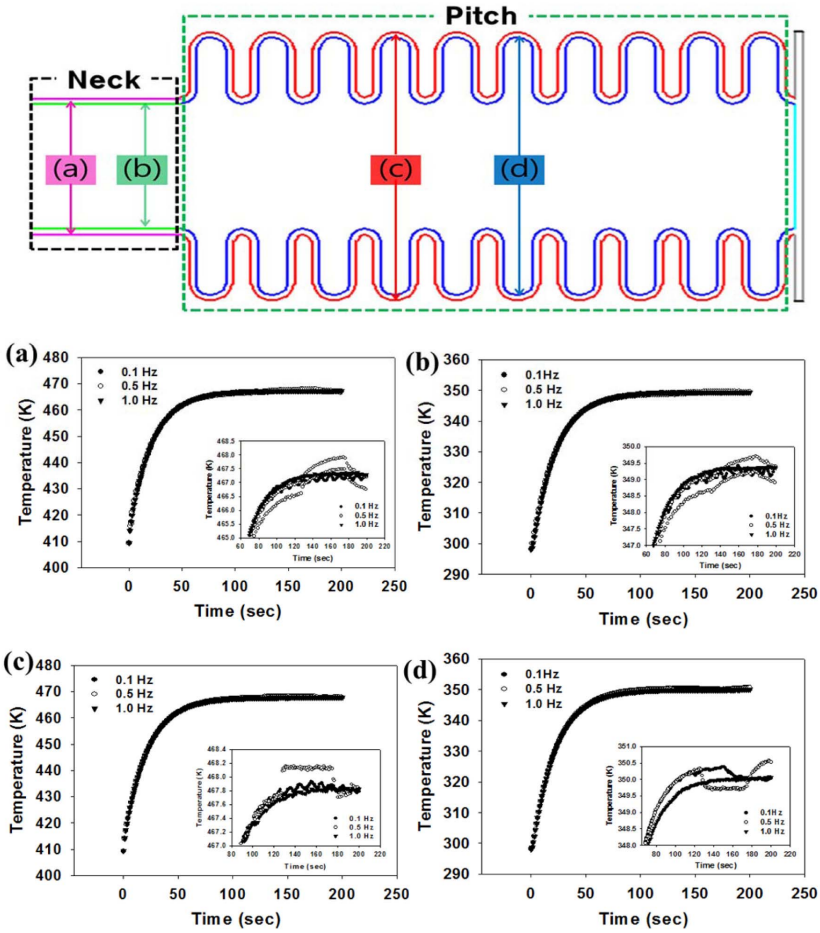


Fig. 5. Profiles of Temperature at Neck and Pitch of Bellows for 200 sec: (a) Temperature Distribution of Neck Surface Facing Sulfuric Acid, (b) of Neck Surface Facing Cooling Water, (c) of Pitch Surface Facing Sulfuric Acid, and (d) of Pitch Surface Facing Cooling Water.

a maximum velocity of 1.418 m/s was observed at the central position located within the bellows end-plate and the check valve. At 0.5 Hz, the velocity distribution within the bellows box was in the range of $8.09 \times 10^{-5}$ - 0.869 m/s. Upon exposure to the cooling water, the velocity distribution was in the range of $8.09 \times 10^{-5}$ - 2.02 m/s. The maximum velocity of 0.869 m/s was observed at the central point within the bellows end-plate and the check valve, which closely resembles the results obtained at 0.1 Hz. At 1.0 Hz, a velocity distribution range of $1.94 \times 10^{-4}$ - 1.129 m/s was observed within the bellows box, while the velocity distribution for the side of coolant was in the range of $1.94 \times 10^{-4}$ - 3.38 m/s. Additionally, the maximum velocity of 1.129 m/s occurred at the center between the bellows end-plate and the bellows box. The maximum expansion point within the bellows and the maximum velocity vastly differed with respect to the frequency, which implied that the velocity did not exhibit a linear relationship with the frequency. The difference in the maximum velocity at each frequency was in the range of 0.22-0.549 m/s.

For the maximum shrinkage point within bellows (Fig. 6 (b)) at 0.1 Hz, the velocity distribution within the bellows box was in the range of $8.09 \times 10^{-5}$ - 1.089 m/s and the range of $8.09 \times 10^{-5}$ - 2.72 m/s within the cooling water portion. This value is the completion point for the absorbance of the hot sulfuric acid. The maximum velocity was 1.089 m/s at all positions including the central position of the bellows box, bellows end-plate, and surrounding bellows. At 0.5 Hz, the velocity distribution within the bellows box was in the range of $1.02 \times 10^{-4}$ - 0.620 m/s and in the range of $1.02 \times 10^{-4}$ - 2.07 m/s for the cooling water portion. The maximum velocity was 0.620 m/s at all positions including the central position of the bellows box, the bellows, and the area surrounding the bellows end-plate. At 1.0 Hz, the velocity distribution within the bellows box was in the range of $4.34 \times 10^{-4}$ - 0.893 m/s with the maximum velocity of 0.893 m/s at the central position of the bellows box and the bellows end-plate. The velocity of the cooling water portion was in the range of $4.34 \times 10^{-5}$ - 3.34 m/s. At the maximum shrinkage point of the bellows, the maximum velocity exhibited no correlation with the frequency. Additionally, the difference in the maximum velocity at each frequency was in the range of 0.196-0.469 m/s.

As the above results, in both cases (expansion or contraction of bellows), flow rate distribution of sulfuric acid was slower than the velocity of cooling water. The heat of high temperature sulfuric acid flowing into bellow was not fast delivered to the bellows box and bellows and flowed out due to slow flow. So, the effect to raise the temperature of bellows was limited. On the other hand, inlet cooling water was fast contacted with the bellows and discharged rapidly due to the fast flow of cooling water, so the cooling effect of the bellows increased.

Regardless of the frequency, the inner flow of the bellows box with respect to the expansion/contraction of the bellows was distinguished by the small flow because of the corrugated pipe and the large flow because of the bellows end-plate. The large flow occurred in the bellows box and was not influenced by the small flow generated by the corrugated pipe. This was caused by a different velocity that was generated by the bellows end-plate and the flow within the bellows, which subsequently formed a vortex.

## 3.2 Simulation Results for the Bellows End-plate

As shown in Fig. 7 (a) though Fig. 7 (c), the temperature distributions are represented as contour images at each condition for 50, 100, 150, and 200 s under all simulated

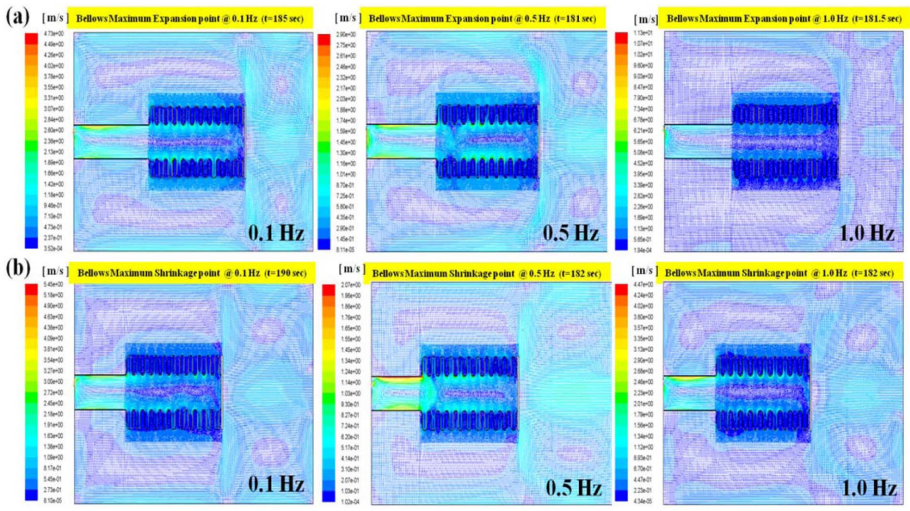


Fig. 6. Velocity Vector of Inside Bellows Box and Moving Part Surrounding Bellows: (a) The Maximum Expansion Point of Each Frequency (0.1, 0.5, and 1.0 Hz) and (b) The Maximum Shrinkage Point of Each Frequency (0.1, 0.5, and 1.0 Hz).

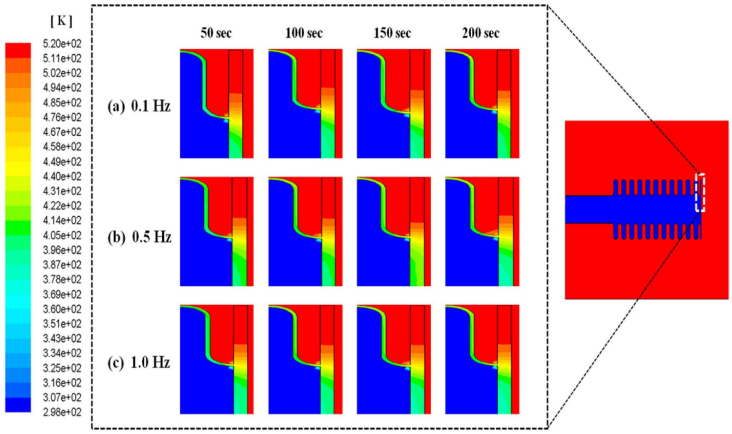


Fig. 7. Temperature Distribution of Bellows End-plate (0.1, 0.5, and 1.0 Hz).

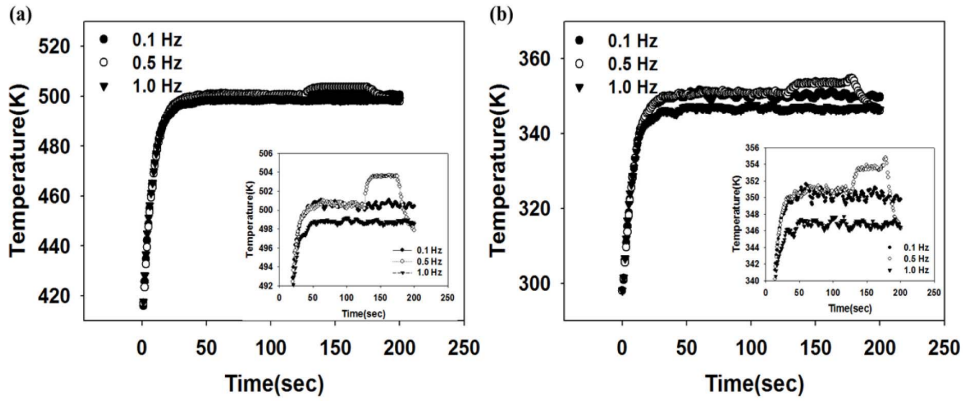


Fig. 8. Temperature Profiles of the Bellows End-plate for 200 sec: (a) Temperature Distribution of Bellows end-plate Surface Facing Sulfuric Acid and (b) Temperature Distribution of Bellows End-plate Surface Facing Cooling Water.

conditions (0.1, 0.5, and 1.0 Hz). The contact surface temperature within the bellows end-plate was in the range of 386-442 K, regardless of the frequency and time. Additionally, this portion was surrounded by hot sulfuric acid in the range of 453-520 K.

As shown in the above results, the temperature distribution was maintained at 50 s in the interior of the bellows end-plate and the surface in contact with the sulfuric acid. This result was caused by the high thermal conductivity of the STS used in the bellows end-plate.

When comparing the results shown in Fig. 4 (a) through Fig. 4 (c), it is evident that 100 s was required to maintain the temperature within the bellows at 0.1, 0.5, and 1.0 Hz; however, less than 50 s was required for the temperature of the interior of the bellows end-plate to reach a constant value. This result is attributed to the different material properties of the applied simulation such that a thermal analysis was required to determine the outcome of various materials being mixed together under high temperatures.

Additionally, as the frequency increased, the various temperature zones were narrowly observed with respect to the position of the bellows end-plate. It was determined that the round trip of the bellows increased as the frequency increased because the heat exchanged relatively quickly at the point between the bellows end-plate and the cooling water. The cooling water quickly recovered the conduction heat radiating from the exterior of the bellows end-plate.

Fig. 8 shows the temperature profiles of the bellows end-plate. Fig. 8 (a) and Fig. 8 (b) show the temperature of the contact surface of the bellows end-plate in contact with the hot sulfuric acid and the cooling water. These values were obtained by monitoring the area-weighted average total temperature every 1 s. The temperature of the contact surface between the bellows end-plate and the hot sulfuric acid increased to 498 K and was maintained at 498 ± 2 K (30, 29, and 43 s were respectively required at 0.1, 0.5, and 1.0 Hz to increase to 498 K). The temperature of the contact surface between the bellows end-plate and the cooling water increased to 346 K and was maintained at 346 ± 7 K. The time for the temperature to increase to 346 K was 21 s at 0.1 Hz, 21 s at 0.5 Hz, and 31 s at 1.0 Hz.

When comparing the results shown in Fig. 5 (a) - Fig.

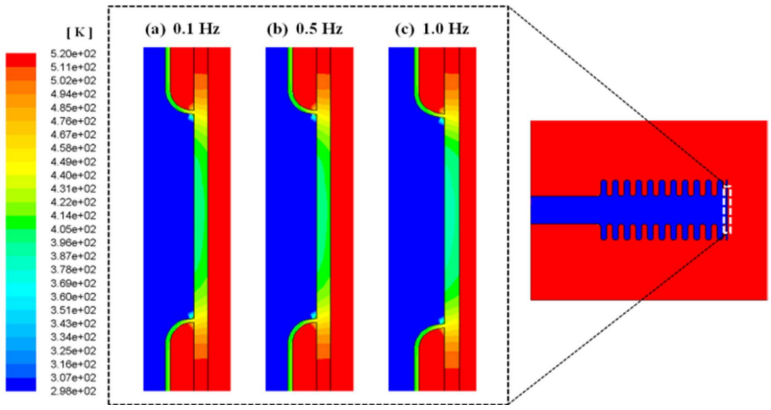


Fig. 9. Temperature Distributions of Contact Position Placing between Bellows (PTFE) and Bellows end-plate at 200 sec.

5 (d), it is evident that the temperature of the contact surface between the bellows (Neck and Pitch) containing the PTFE with the hot sulfuric acid was 453 K (0.1 Hz, 30 s), 453 K (0.5 Hz, 29 s), and 459 K (1.0 Hz, 43 s). Additionally, the temperature of the surface in contact with the cooling water was 341 K (0.1Hz, 42 s), 338 K (0.5 Hz, 35 s), and 336 K (1.0 Hz, 31 s).

The bellows end-plate was composed of STS and its thermal conductivity was higher than that of PTFE. Therefore, the conduction heat transferred from the hot sulfuric acid quickly transmitted to the cooling water. This phenomenon prevented the deformation of the bellows end-plate upon exposure to high temperatures.

### 3.3 Simulation Results for the Conjunction between the Bellows and the End-plate

Fig. 9 shows the temperature distributions of the contact position between the bellows (containing PTFE) and the bellows end-plate when calculation time was 200 s at 0.1, 0.5, and 1.0 Hz. The temperature, measured at the point of contact between the PTFE of the bellows and the portion of the bellows end-plate composed of STS, was in the range of 420-464 K at all frequencies. The temperature (420 K) of the bellows was significantly lower than that of the bellows end-plate (464 K) by 44 K. Based on these results, it is likely that the deformation of the portion between the PTFE and STS materials would not occur, despite the two materials exhibiting different physical/thermal properties.

However, at the initial condition, if we assume that the hot sulfuric acid (520 K) filled the entire bellows box, the cooling water (298 K) filled the interior of the bellows, and the temperature was constant within the bellows and the bellows end-plate, then the maximum temperature difference between the hot sulfuric acid and the cooling water will be 222 K. This is because the temperature of the surface in contact with the hot sulfuric acid was 520 K and the temperature of the surface in contact with the cooling water was 298 K.

In this study, it was determined that it is necessary to physically reinforce the connection parts and eliminate the temperature difference of 222 K to enable the use of bellows and bellows end-plate in the acid transfer system. Therefore, we plan to carry out additional studies on the structural analysis and stress analysis of the bellows and the bellows end-plate.

## 4. CONCLUSIONS

A CFD analysis for the bellows and the bellows end-plate portions of the transfer system was conducted. The main systems used to transfer hot sulfuric acid consisted of a bellows box, a bellows, and an end-plate of the bellows. When the newly proposed transfer system design was implemented, the temperature of the inner bellows (PTFE) increased up to 420 K as the frequency increased and was kept constant at ~420 K. However, the time required to reach the maximum temperature was different at each frequency.

Based on the temperature (420 K) within the bellows, we identified a temperature difference of ~180 K relative to the melting point of PTFE (600 K). This result indicates that PTFE can be used as a structural material for the bellows in the sulfuric acid transfer pump during the SI process. The temperature distribution within the bellows end-plate (STS) was in the range of 386-520 K and various regions appeared narrow as the frequency increased at the same position. The temperature distribution of the surface in contact with the cooling water was in the range of 386-422 K, while the temperature distributions of the surface in contact with the hot sulfuric acid was in the range of 453-520 K. The temperature of the bellows surface in contact with the hot sulfuric acid increased to 467 K and was maintained at 467 ± 2 K at all frequencies. The temperature of the surface in contact with the cooling water reached 349 K and was maintained at 349 ± 2 K at all frequencies.

Also, in both cases (expansion or contraction of bellows), flow rate distribution of sulfuric acid was slower than the velocity of cooling water. The effects for heat of sulfuric acid raising temperature of bellows was not significant, rather than the rapid flow of cooling water was a greater effect because it fast absorbed the heat of bellows and discharged.

The results presented herein are the first data simulating the heat transfer characteristics of the transfer system for hot sulfuric acid using PTFE. We believe that these results will contribute to the optimization of the transfer system used for transporting sulfuric acid.

## ACKNOWLEDGEMENTS

This work was supported by the National Research Foundation of Korea (NRF) grant funded by the Korean government (MSIP) (No. 53154-14)

## REFERENCES

[1] Richa Kothari, D. Buddhi, R.L. Sawhney, "Sources and technology for hydrogen production: a review", International Journal of Global Energy Issues, Vol. 21, pp. 154-178 (2004).

[2] J. E. Funk, R. M. Reinstrom, "Energy Requirements in Production of Hydrogen from Water", Industrial & Engineering Chemistry Process Design and Development, Vol. 5(3), pp. 336–342 (1966). (DOI: 10.1021/i260019a025)

[3] K. Onuki, S. Shimizu, H. Nakajima, S. Fujita, Y. Ikezoe, S. Sato, S. Machi, "Studies on an iodine–sulfur process for thermochemical hydrogen production", Proceeding of the 8th World Hydrogen Energy Conference, Honolulu, pp. 547–556 (1990).

[4] H. Nakajima, K. Ikenoya, K. Onuki, S. Shimizu, "Closed-Cycle Continuous Hydrogen Production Test by Thermochemical SI Process", Kagaku Kogaku Ronbunshu, Vol. 24(2), pp. 352-355 (1998). (in Japanese)

[5] M. Sakurai, H. Nakajima, K. Onuki, K. Ikenoya, S. Shimizu, "Preliminary process analysis for the closed cycle operation of the iodine–sulfur thermochemical hydrogen production process", International Journal of Hydrogen Energy, Vol. 24(7), pp. 603–612 (1999).

[6] Norman, J. H., Besenbruch, G. E., Brown, L. C., O'Keefe, D. R., Allen, C. L., "Thermochemical water-splitting cycle, bench-scale investigations, and process engineering. Final report, February 1977-December 31, 1981", Technical Report, GA-A-16713 (1982).

[7] Norman, J. H., G. E. Basenbruch, D. R. O'keefe, "Thermochemical water-splitting for hydrogen production", GRI-80/0105 (1981).

[8] G. E. BESENBRUCH, L. C. BROWN, J. F. FUNK, S. K. SHOWALTER, "HIGH EFFICIENCY GENERATION OF HYDROGEN FUELS USING NUCLEAR POWER", General Atomic Project 30047, GA–A23510 (2000).

[9] Seiji Kasahara, Gab-Jin Hwang, Hayato Nakajima, Ho-Sang Choi, Kaoru Onuki, Mikihiro Nomura, "Effects of Process Parameters of the IS Process on Total Thermal Efficiency to Produce Hydrogen from Water", JOURNAL OF CHEMICAL ENGINEERING OF JAPAN Vol. 36(7), Special Issue for Energy Engineering, pp. 887-899 (2003).

[10] Dokiya, M., Kameyama, T., Fukuda, K., Kotera, Y., "The study of thermochemical hydrogen preparation. III. An oxygenevolving step through the thermal splitting of sulfuric acid", Bulletin of The Chemical Society of Japan, Vol. 50(10), 2657-2660 (1977).

[11] D. R. O'keefea, J. H. Normana, D. G. Williamson, "Catalysis Research in Thermochemical Water-Splitting Processes", Catalysis Reviews: Science and Engineering, Vol. 22(3), pp. 325-369 (1980).

[12] V. Barbarossa, S. Brutti, M. Diamanti, S. Sau, G. De Maria, "Catalytic thermal decomposition of sulphuric acid in sulphur–iodine cycle for hydrogen production", International Journal of Hydrogen Energy, Vol. 31(7), pp. 883–890 (2006).

[13] Ginosar, D. M., Glenn, A. W., Petkovic, L. M., "Stability of Sulfuric Acid Decomposition Catalysts for Thermochemical Water Splitting Cycles. Paper 76b, AIChE 2005 Spring National Meeting Overall Conference Proceedings (2005).

[14] Onuki, K., Ioka, I., Futakawa, M., Nakajima, H., Shimizu, S., Tayama, I., "Screening Tests on Materials of Construction for the Thermochemical IS Process", CORROSION ENGINEERING, Vol. 46(2), pp. 141-149 (1997).

[15] Daniel M. Ginosar, Lucia M. Petkovic, Kyle C. Burch, "Activity and stability of sulfuric acid decomposition catalysts for thermochemical water splitting cycles", American institute of chemical engineers national meeting. Cincinnati, OH. Paper 285d (2005).

[16] A. Giaconia, G. Caputo, A. Ceroli, M. Diamanti, V. Barbarossa, P. Tarquini, S. Sau, "Experimental study of two phase separation in the Bunsen section of the sulfur–iodine thermochemical cycle", International Journal of Hydrogen Energy, Vol. 32(5), pp. 531–536 (2007).

[17] Stephen Goldstein, Jean-Marc Borgard, Xavier Vitart, "Upper bound and best estimate of the efficiency of the iodine sulphur cycle", International Journal of Hydrogen Energy, Vol. 30(6), pp. 619–626 (2005).

[19] L. C. BROWN, R. D. LENTSCH, G. E. BESENBRUCH, K. R. SCHULTZ, J. E. FUNK, "ALTERNATIVE FLOWSHEETS FOR THE SULFUR-IODINE THERMOCHEMICAL HYDROGEN CYCLE", GA–A24266, pp. 1-14 (2003).

[20] Sauer-Danfoss Company, "Series 90 Axial Piston Pumps Technical Information", 520L0603(Rev. FC), pp. 9 (2008).

[21] DuPont Fluoroproducts, "Properties Handbook, Teflon ® PTFE", 220313D, pp. 1-34.

[22] ANSYS Inc., Fluent 14.5 User's Guide, Canonsburg, PA, USA (2013).

[23] ANSYS Inc., Fluent 14.5 UDF Manual, Canonsburg, PA, USA (2013).

[24] L. C. BROWN, G. E. BESENBRUCH, R. D. LENTSCH, K. R. SCHULTZ, J. F FUNK, P. S. PICKARD, A. C. MARSHALL, S. K. SHOWALTER, "HIGH EFFICIENCY GENERATION OF HYDROGEN FUELS USING NUCLEAR POWER FINAL TECHNICAL REPORT FOR THE PERIOD AUGUST 1, 1999 THROUGH SEPTEMBER 30, 2002", General Atomics Report GA–A24285, Rev. 1, pp. 3-6 ~ 3-21 (2003)

[25] ANSYS Inc., Fluent 14.5 Theory Guide, Canonsburg, PA, USA (2013).

[26] http://en.wikipedia.org/wiki/Polytetrafluoroethylene

[27] The European Stainless Steel Development Association, "Stainless Steel: Tables of Technical Properties", Materials and Applications Series, Volume 5, pp. 18 (2007).